Detection and Attribution of Climate Non-Stationarity in Cold Regions Geotechnical Design Using Artificial Intelligence

Elham Kheradmand[1], Ali Fatolahzadeh Gheysari[2], Parisa Samadi[3], Sina Javankhoshdel[4], Terence Ma[4], Kien Dang[4], Dipanjan Basu[5], and Pooneh Maghoul[6(✉)]

[1] Université de Montréal, Montreal, QC, Canada
[2] University of Manitoba, Winnipeg, MB, Canada
[3] Iran University of Science and Technology, Tehran, Iran
[4] Rocscience Inc, Toronto, ON, Canada
[5] University of Waterloo, Waterloo, ON, Canada
[6] Polytechnique Montreal, Montreal, QC, Canada
pooneh.maghoul@polymtl.ca

Abstract. As our climate changes (non-stationarity), we face new challenges in assessing hazard frequency and assessing the vulnerability of infrastructure to the effects of global warming, such as changing precipitation patterns and increasing ground surface temperature. The lack of appropriate incorporation of future weather and climate information into the design, operation, and management of infrastructure remains a significant barrier to systematically improving climate-resilient infrastructure. In this paper, a spatiotemporal AI-powered platform for the detection and attribution of climate non-stationarity is used to as boundary conditions in a computational simulator to investigate the resiliency of a typical embankment in Canada. It can be seen that considering the climate boundary condition causes the reduction in the factor of safety of the embankment and the change of the performance of the geosynthetic layer under the embankment.

1 Introduction

Many geotechnical engineering projects require information on ground temperature profiles, especially in cold climates. For instance, to choose the suitable burial depth for utilities to prevent freezing, the annual variation of the ground temperature profile can play a significant role. Also, it has an impact on the thermal performance of shallow geothermal systems. Moreover, it is an indicator for possible permafrost thaw that can adversely affect the structural integrity of northern infrastructure such as pipelines, roads, and so on. By 2050, permafrost degradation will have a negative impact on nearly 70% of the arctic infrastructure, costing between $21 billion and $43 billion annually in Canada as a result of the severe consequences of climate change [1, 2]. Therefore, assessing the ground temperature profile and forecasting future changes over the service life of construction projects are critical elements in developing a sustainable and climate-smart geotechnical design.

R. E. Hammah et al. (Eds.): RIC 2023, AHE 19, pp. 325–336, 2023.
https://doi.org/10.2991/978-94-6463-258-3_34

Ground Surface Temperature (GST) is frequently utilised in the evaluation of freeze-thaw-induced frost action such as frost heave, thaw settlement, and winter road operation.

The GST is frequently determined using physics-based procedures, i.e., by solving the surface energy budget (SEB) using analytical or numerical methods. For this purpose, it is necessary to include all of SEB's contributing factors, including air convection heat fluxes at the ground surface, solar radiation, and the insulating effects of snow cover [3]. Weather station records can be used to determine the inputs of the model, including air temperature and snow depth, to compute either the current or previous GST. Nevertheless, inputs that take into account future climatic patterns are needed for long-term physics-based GST forecasting. Climate models give forecasts of meteorological variables that may be utilised as boundary conditions in SEB analysis to compute GST under various climatic paths. The spatial resolution of certain global climate models, such as the Canadian Earth System Model (CanESM), is 2.8° (more than 300 km) [4] at the time of this study, which is inadequate in many applications. Nonetheless, the CanESM predicts temperatures near the ground surface.

While physics-based analysis of the surface energy budget (SEB) is the most precise method for determining ground temperature, its application in real-world scenarios is limited due to various challenges. SEB involves numerous components, physics, and site-specific factors that require detailed modelling and multiple inputs of the land-atmosphere energy system. Any omission of a component can significantly impact the results, and SEB's multiphysics simulation is computationally demanding. Thus, simulating a geospatial mesh grid at small temporal increments becomes impractical for multi-decade research periods. Therefore, the Ground Surface Temperature (GST) is frequently calculated using meteorological data without SEB analysis. One of the commonly used techniques is the n-factor method, which determines the mean seasonal GST from air temperature and the number of days with freezing or above-zero temperatures in the soil and air. However, this approach has limitations, such as not considering other SEB components that can impact ground temperature and being influenced by long-term climatic changes and interannual variations in air temperature. Thus, it is unsuitable for GST forecasting. However, advancements in data management and machine learning algorithms have made data-driven forecasting systems advantageous. With the increasing trend of data collection and storage, data can be analyzed for correlations, patterns, and trends. Artificial neural networks (ANN) and regression analysis can be used to calculate the GST from measurements of air temperature and other meteorological variables, as previously demonstrated. Such data-driven approaches provide a promising alternative to SEB analysis and can facilitate GST forecasting with improved accuracy and efficiency. [5].

The ground's thermal mass causes the temperature below the surface to lag behind the air temperature [11–13]. The GST is also affected by previous climatic conditions due to above- and below-surface heat fluxes such as solar radiation and air convection at the ground surface. This has been partially addressed by including the previous climatic conditions in the input characteristics of artificial neural networks (ANN). In other words, each item in the training and test input sets can represent a previous series of input parameters [14]. While this method has considerably increased estimation accuracy, ANNs treat data as X-Y points and not as a time series. Linear stochastic approaches,

such as autoregressive integrated moving averages (ARIMA), have also been attempted to predict the GST. However, this technique only considers historical trends in soil temperature time series and ignores the controlling SEB components, making it unsuitable for long-term GST forecasting.

Recurrent neural networks (RNNs) are a type of neural network specifically designed to analyze time series data and capture temporal dynamics. Because RNNs have a chain-like structure of repeated cells in a temporal sequence, the output of one step can influence the output of subsequent stages. This enables RNNs to store information and analyze inputs sequentially. However, when the input sequence is lengthy, backpropagation across time in RNNs can lead to vanishing or exploding gradients. Specialized RNN types that address this issue include long short-term memory (LSTM), gated recurrent unit (GRU), and their derivatives, which can handle longer sequences [16]. LSTMs have been successfully applied in various climate and earth science investigations, such as forecasting rainfall, sea surface temperature, and restoring missing groundwater level data [17–19]. In recent literature, there has been discussion of using LSTMs to estimate GST from meteorological forcings [20]. However, the two-year training dataset used in these studies may not adequately represent the interannual variability of weather, and the accuracy of estimates at different times of the year, such as during different seasons and yearly peaks, is unknown. Recently, Gheysari et al. [21] developed an LSTM-based data-driven method for forecasting ground surface temperature by utilizing past ground and air temperatures, along with other meteorological measurements. The framework is flexible and can incorporate various components of the surface energy budget if they have been previously measured at the site. By considering different climate change scenarios, the model can predict ground surface temperature under different projections of meteorological variables without requiring additional computation. Additionally, the framework inherently captures the underlying drivers of climate scenarios, which are reflected in the predicted ground surface temperature.

A significant obstacle to systematically enhancing climate-resilient infrastructure is the inadequate incorporation of future weather and climate information into the design, operation, and management of infrastructure, particularly at spatiotemporal scales pertinent to particular engineering problems. The present study uses a spatiotemporal AI-powered platform developed by Gheysari et al. [21] to identify and attribute climatic non-stationarity in a site. This projection is then utilised as the boundary conditions in a computational simulator to study the resilience of a typical Canadian embankment [21].

2 Data Feature Analysis

Our historical annual dataset includes GST measurements spanning from 1950 to 2021. Based on this data, we have generated predictions for the years 2006 through 2100. Figure 1 presents the annual measurements for historical and predicted surface temperatures. Based on the information presented in Fig. 1, it is evident that there is a trend of increasing annual surface temperatures in the future.

The annual GST shows that the data is non-stationary. To verify the non-stationarity of the annual temperature data, we conducted an Augmented Dickey-Fuller (ADF) test. A series is non-stationary if its statistical properties such as the mean and variance

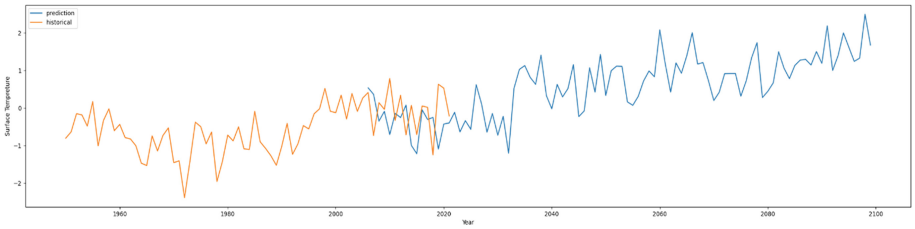

Fig. 1. The illustration of the annual surface temperature for the historical and prediction data [21]

Table 1. Observations of the Augmented Dickey-Fuller test for annual prediction data

	Annual
Test Statistic	−1.170768
p-value	0.686042
critical value (1%)	−3.506057
critical value (5%)	−2.894607
critical value (10%)	−2.584410

change over time. In the ADF test, a test statistic and a p-value are generated. If the p-value is less than a pre-determined significance level, typically 0.05, we reject the null hypothesis of non-stationarity and conclude that the data is stationary. If the p-value is greater than the significance level, we fail to reject the null hypothesis and conclude that the data is non-stationary. Table 1 presents the results of the hypothesis tests conducted on the annual prediction values. The p-value for the annual prediction value is 0.69, which exceeds the significance level of 0.05. The test statistic for the annual prediction data is −1.17, which exceeds all the critical values. These results provide evidence that the annual data is non-stationary.

Furthermore, Fig. 2 displays the historical and predicted annual surface temperature data for each month, spanning every 10 years from 1950. The figure reveals that surface temperatures are projected to increase in the future, particularly in July 2060. Notably, there is a significant difference between the predicted temperatures for June, with the predicted temperature being higher than the other temperatures, and this difference is particularly pronounced in 2060.

3 Effects of Climates on Slope Stability

3.1 Problem Description

This example presents the effects of climate on slope stability. The climate boundary condition were selected from the Nunavik region presented in the previous section. An embankment underlain by a foundation is modelled. Three different cases are considered

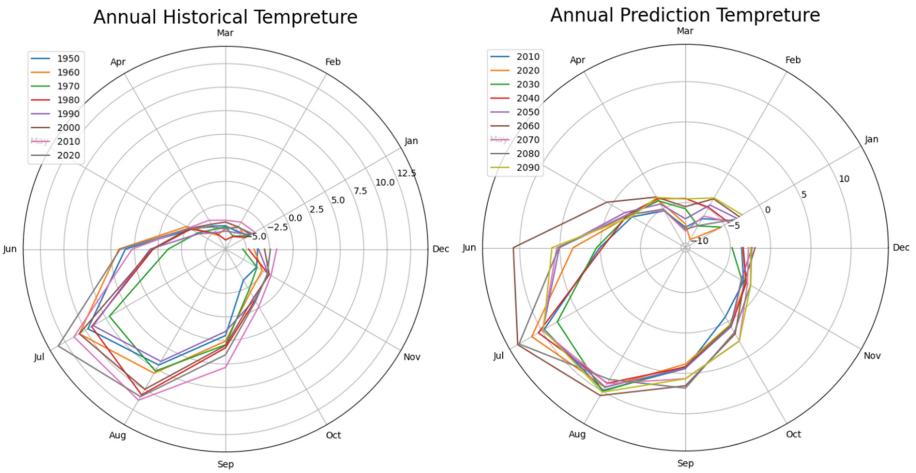

Fig. 2. The illustration of the radar plot for the historical (left) and prediction (right) surface temperature data

in this example. The first one is the model that has no geosynthetic. The second one has geosynthetic installed to increase the shear strength reduction factor (SRF) from 1.15 to 1.25 by adding the geosynthetic layer under the embankment. The last case monitors the climate effect over time. Comparing the results for all three cases, the impact of climate effect on slope stability can be observed.

Note that the SRF is a metric which predicts the stability of the slope using the finite element method. In determining the SRF, the material shear strength is gradually reduced until the loss of numerical convergence occurs in FE (indicating that the slope has mobilized). The SRF is the reduction factor which corresponds to the instability, and as such, is analogous to the factor of safety for slope stability.

Model Geometry

The model used in this study comprises of a foundation layered by five types of clay. The foundation is 24 m in height and 90 m in width. The sloped embankment on top of the foundation consists of four materials, with a 1 m-thick first layer. The embankment is 5 m height and 50 m width in total, with slopes on both sides.

Case 1: No geosynthetic, no climate effects (Fig. 3).

Case 2: A geosynthetic with joints as slip on both sides is added as a structural interface in RS2. The geosynthetic is applied to the top of the lower embankment layer. Note that the thermal effect on geosynthetic including the thermal expansion is considered in this model (see Table 4). No climate effects are assumed in this case (Fig. 4).

Case 3: A geosynthetic is included in the same way as in model 2. Thermal boundary conditions are applied to account for the climate effect on slope stability. The analysis is taken over 150 years, which initially started in 1950. Two sets of data as discussed in the previous section were used in the numerical analysis. From the year 1950 to 2006 the historical data was used and from 2006 to 2100 the predicted data is used in the model. The total of 15 stages were defined in regular intervals over 150 years. A transient thermal boundary condition is applied to the model as it can be seen in Fig. 5

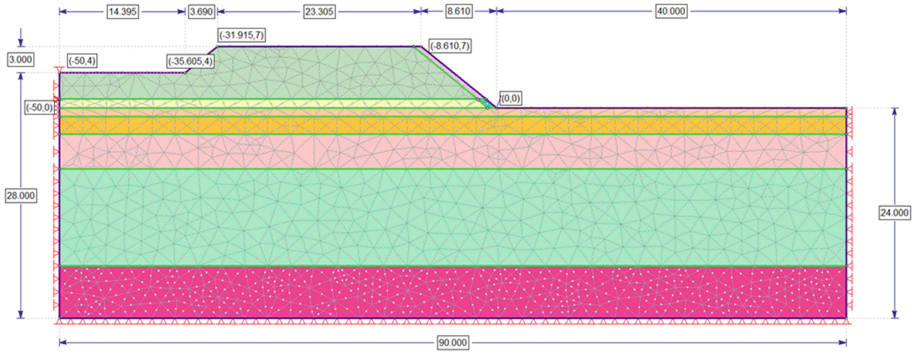

Fig. 3. Case 1 geometry

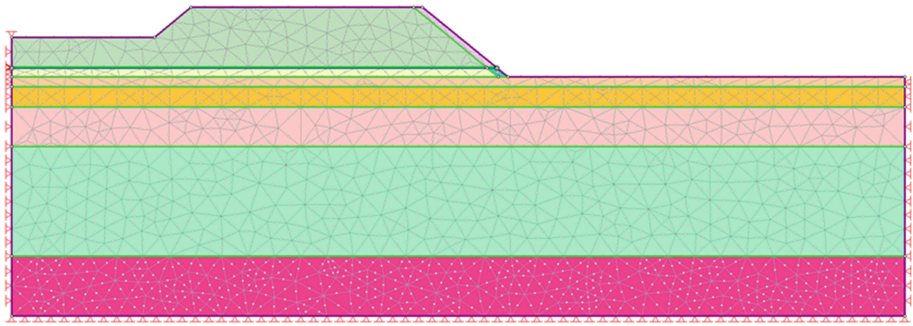

Fig. 4. Case 2 geometry

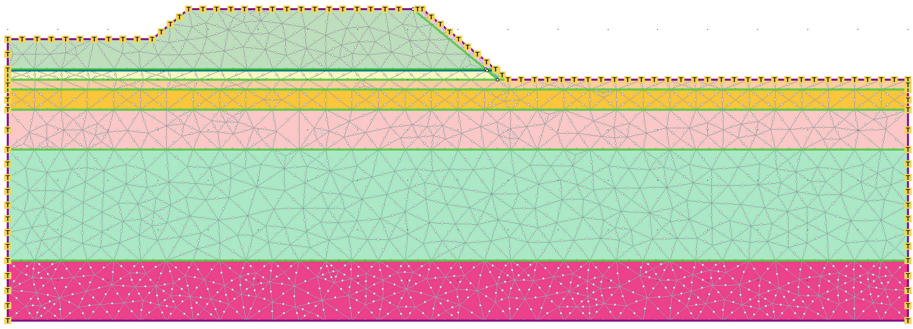

Fig. 5. Case 3 geometry and thermal boundary conditions.

3.2 Material Properties

The material properties are shown in Tables 2 to 3. The RS2 software was used to perform the shear strength reduction analysis.

The geosynthetic properties are given in Table 4. The liner properties on both sides of the geosynthetic are given in Table 5.

Table 2. Mechanical properties

		Emban-kment upper	Embank-ment upper elastic	Embank-ment lower	Embank-ment lower elastic	Clay 1	Clay 2	Clay 3	Clay 4	Clay 5
Initial element loading		Field stress and body force								
Unit weight (kN/m3)		21.9	21.9	17.2	17.2	18	17.5	13.5	17	17.5
Porosity value		0.5	0.5	0.5	0.5	0.5	0.5	0.5	0.5	0.5
Poisson's ratio		0.4	0.4	0.4	0.4	0.4	0.4	0.4	0.4	0.4
Young's Modulus (kPa)		50 000	50 000	50 000	50 000	50 000	50 000	50 000	50 000	50 000
Failure criterion		Mohr-Coulomb								
Material type		Plastic	Elastic	Plastic	Elastic	Plastic	Plastic	Plastic	Plastic	Plastic
Peak strength	Peak tensile strength (kPa)	0	0	0	0	43	31	30	32	32
	Peak friction angle (degrees)	35	35	33	33	0	0	0	0	0
	Peak cohesion	0	0	0	0	43	31	30	32	32
Residual strength	Residual friction angle (degrees)	35	N/A	33	N/A	0	0	0	0	0
	Residual cohesion (kPa)	0	N/A	0	N/A	43	31	30	32	32
	Dilation angle (degrees)	0	N/A	0	N/A	0	0	0	0	0
	Apply SSR	Yes	N/A	Yes	N/A	Yes	Yes	Yes	Yes	Yes

Table 3. Thermal properties

Material name	Thermal Conductivity	Quartz content	Thermal heat capacity	Include latent heat	Soil specific heat capacity (kJ/ton/C)
Embankment upper	Johansen	0.74	Jame Newman	No	500
Embankment upper elastic	Johansen	0.74	Jame Newman	No	500
Embankment lower	Johansen	0.74	Jame Newman	No	755
Embankment lower elastic	Johansen	0.74	Jame Newman	No	500
Clay 1	Johansen	0.74	Jame Newman	Yes	755
Clay 2	Johansen	0.74	Jame Newman	Yes	755
Clay 3	Johansen	0.74	Jame Newman	Yes	755
Clay 4	Johansen-Lu	0.74	Jame Newman	Yes	755
Clay 5	Johansen-Lu	0.74	Jame Newman	Yes	755

Table 4. Geosynthetic properties

Parameter	Value
Liner type	Geosynthetic
Geosynthetic unit weight (kN/m)	0.05
Initial Temperature (C)	2
Reinforcement type	ACE Geosynthetics – ACE Grid GG30-I
Tensile modulus (kPa)	200,000
Material type	Plastic
Tensile strength (peak) (kN/m)	300
Thermal properties	
Activate thermal	Yes
Conductivity (kW/m/C)	0
Specific heat capacity (kJ/ton/C)	1
Thermal expansion	Yes
Expansion coefficient	0.00017

Table 5. Joints properties

Parameter	Value
Slip criterion	Mohr-Coulomb
Peak friction angle (°)	30.96

4 Results

Figures 6, 7, 8, 9 and 10 show the maximum shear strain contours for each case, and the axial force along the geosynthetic in cases 2 and 3. Applying the climate boundary conditions, the geosynthetic shrank and created more tension along the geosynthetic, it excesses the capacity of 300, the capacity reduced to residual value of 0 at the middle section of geosynthetic (Fig. 10). Thus. The SRF further reduced to 1.15 compared to the case with no climate boundary condition (SRF = 1.25) and the same as the case that we have no reinforcement for the slope.

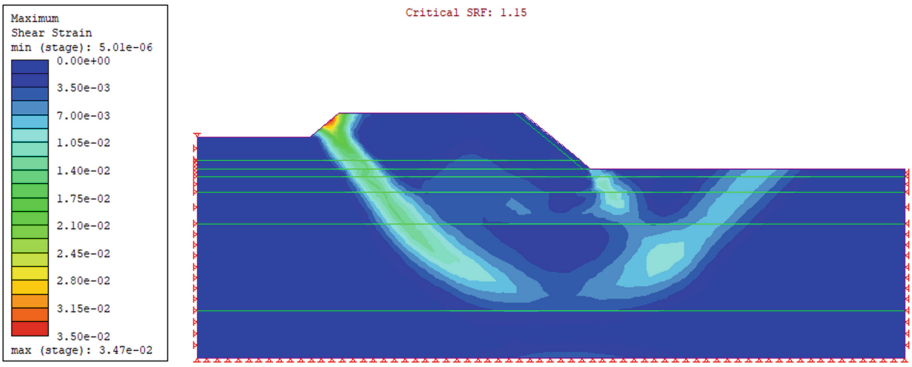

Fig. 6. Model 1 (no geosynthetic)

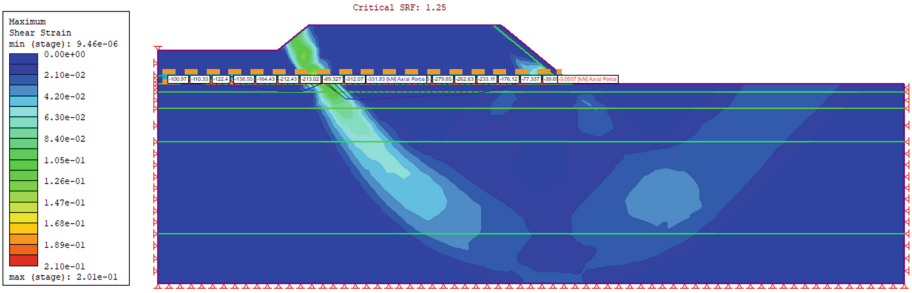

Fig. 7. Model 2 (no climate)

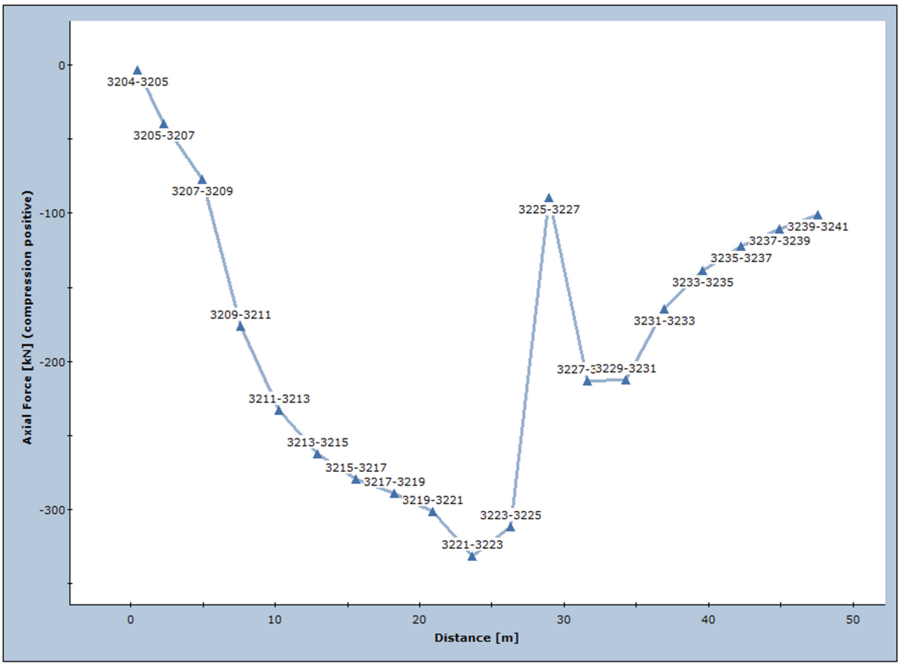

Fig. 8. Case 2 (no climate), axial force along geosynthetic

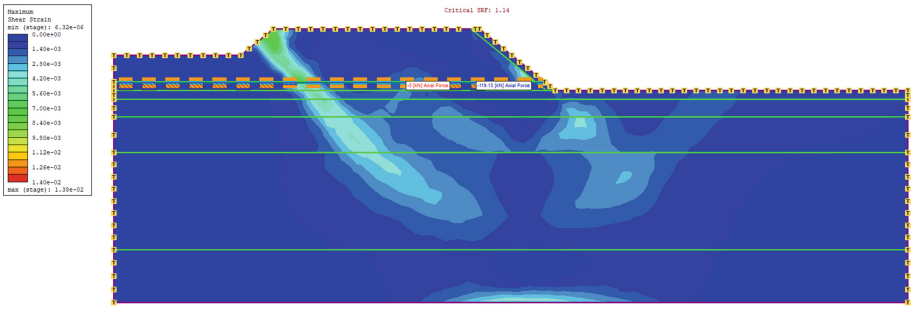

Fig. 9. Case 3

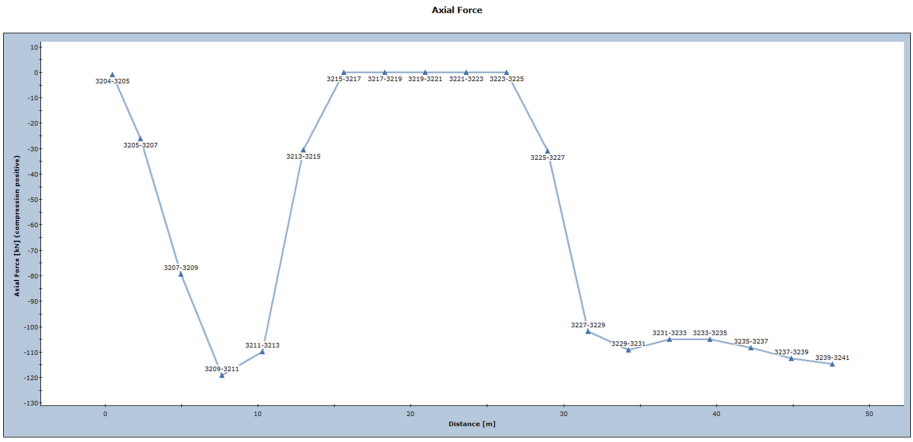

Fig. 10. Case 3, axial force along geosynthetic

5 Conclusion

Climate change is an important consideration for engineering design in geotechnical problems. As demonstrated in this study, the effect of climate change can potentially cause rises in ground temperatures and reductions to the stability of slopes such as embankments. As prediction models continue to become prevalent in the industry, this study has presented the use of an LSTM neural network for predicting the changes in ground temperatures over time. The finite element method was employed to establish a thermal simulation for the evaluation of slope stability in a simple embankment. For solving long-term geotechnical problems, practitioners are encouraged to consider the long-term changes to ground conditions due to climate change.

References

1. Legg, S., *IPCC, 2021: Climate change 2021-the physical science basis.* Interaction, 2021. **49**(4): p. 44–45.
2. Environment, N.R.T.o.t. and t. Economy, *Paying the price: The economic impacts of climate change for Canada.* Vol. 4. 2011: National Round Table.
3. Hjort, J., et al., *Impacts of permafrost degradation on infrastructure.* Nature Reviews Earth & Environment, 2022. **3**(1): p. 24–38.
4. Kong, X., G. Doré, and F. Calmels, *Thermal modeling of heat balance through embankments in permafrost regions.* Cold Regions Science and Technology, 2019. **158**: p. 117–127.
5. Smith, M. and D. Riseborough, *Climate and the limits of permafrost: a zonal analysis.* Permafrost and Periglacial Processes, 2002. **13**(1): p. 1–15.
6. Liu, H., et al., *Feasibility study of snow melting system for bridge decks using geothermal energy piles integrated with heat pump in Canada.* Renewable Energy, 2019. **136**: p. 1266–1280.
7. Swart, N.C., et al., *The Canadian earth system model version 5 (CanESM5. 0.3).* Geoscientific Model Development, 2019. **12**(11): p. 4823–4873.

8. Klene, A.E., et al., *The n-factor in natural landscapes: variability of air and soil-surface temperatures, Kuparuk River Basin, Alaska, USA.* Arctic, Antarctic, and Alpine Research, 2001. **33**(2): p. 140–148.
9. Riseborough, D. *Thawing and freezing indices in the active layer*. in *Proceedings of the 8th International Conference on Permafrost*. 2003. Rotterdam: AA Balkema.
10. Tabari, H., A.-A. Sabziparvar, and M. Ahmadi, *Comparison of artificial neural network and multivariate linear regression methods for estimation of daily soil temperature in an arid region.* Meteorology and Atmospheric Physics, 2011. **110**: p. 135–142.
11. Beltrami, H., *On the relationship between ground temperature histories and meteorological records: a report on the Pomquet station.* Global and Planetary Change, 2001. **29**(3–4): p. 327–348.
12. Gilpin, R. and B. Wong, *"Heat-valve" effects in the ground thermal regime.* 1976.
13. Saaly, M., et al., *Energy performance of below-grade envelope of an institutional building in cold regions.* Journal of Building Engineering, 2020. **27**: p. 100911.
14. Barzegar, R., et al., *Exploring the hydrogeochemical evolution of cold and thermal waters in the Sarein-Nir area, Iran using stable isotopes (δ18O and δD), geothermometry and multivariate statistical approaches.* Geothermics, 2020. **85**: p. 101815.
15. Zeynoddin, M., et al., *A reliable linear stochastic daily soil temperature forecast model.* Soil and Tillage Research, 2019. **189**: p. 73–87.
16. Schmidhuber, J. and S. Hochreiter, *Long short-term memory.* Neural Comput, 1997. **9**(8): p. 1735–1780.
17. Kratzert, F., et al., *Rainfall–runoff modelling using Long Short-Term<? xmltex\break?> Memory (LSTM) networks.* Hydrology and Earth System Sciences, 2018. **22**(11): p. 6005–6022.
18. Vu, M., et al., *Reconstruction of missing groundwater level data by using Long Short-Term Memory (LSTM) deep neural network.* Journal of Hydrology, 2021. **597**: p. 125776.
19. Yang, Y., et al., *A CFCC-LSTM model for sea surface temperature prediction.* IEEE Geoscience and Remote Sensing Letters, 2017. **15**(2): p. 207–211.
20. Li, Q., Y. Zhao, and F. Yu, *A novel multichannel long short-term memory method with time series for soil temperature modeling.* IEEE Access, 2020. **8**: p. 182026–182043.
21. Fatolahzadeh Gheysari, A., Maghoul, P., Ashraf, A., Salaby, A. 2022. AI-powered ground surface temperature forecasting for cold regions geotechnical applications, GeoCalgary, 2022.